HYDROGEN EQUIPMENT ENCLOSURE RISK REDUCTION THROUGH EARLIER DETECTION OF COMPONENT FAILURES

K. Hartmann[1], A. Tchouvelev [2], B. Angers [3], J. Thorson[1], A. Al-Douri [4], K. Groth [4], and W. Buttner [1]

1 Energy Conversion and Storage Systems Center, National Renewable Energy Laboratory, 15013 Denver W Pkwy, Golden, CO, 80401, USA, Kevin.Hartmann2@nrel.gov

2 A.V. Tchouvelev & Associates Inc., 6591 Spinnaker Cir, Mississauga, ON, Canada, atchouvelev@tchouvelev.org

3 Hydrogen Research Institute, Université Du Québec à Trois-Rivières, QC, Canada, Benjamin.Angers@uqtr.ca

4 Center for Risk and Reliability, University of Maryland, 0151 Glenn L. Martin Hall, College Park, MD, 20742, USA, kgroth@umd.edu

ABSTRACT

Hydrogen component reliability and the hazard associated with failure rates is a critical area of research for the successful implementation and growth of hydrogen technology across the globe. The research team has partnered to quantify system risk reduction through earlier detection of hydrogen component failures. A model of hydrogen dispersion in a hydrogen equipment enclosure has been developed utilizing experimentally quantified hydrogen component leak rates as inputs. This model provides insight into the impact of hydrogen safety sensors and ventilation on the flammable mass within a hydrogen equipment enclosure. This model also demonstrates the change in safety sensor response time due to detector placement under various leak scenarios. The team looks to improve overall hydrogen system safety through an improved understanding of hydrogen component reliability and risk mitigation methods. This collaboration fits under the work program of IEA Hydrogen Task 43 Subtask E Hydrogen System Safety.

1.0 INTRODUCTION

Developing a better understanding of leak behavior and leak size is a critical step in the development of risk and reliability engineering for hydrogen systems [1]. Making risk informed decisions will play an even more important role as the hydrogen community continues to expand. It is critical to prioritize safety now to avoid safety events which could be detrimental to the growth of hydrogen as a renewable energy storage mechanism. Already, the hydrogen community is working to meet the hydrogen shot 111 initiative to reach a price of $1 per kg in one decade (launched June 2021) [2]. To support this hydrogen shot initiative significant resources are being put into the development and expansion of hydrogen systems. Safety research and regulations codes and standards (RCS) need to grow to continue to provide guidance and best practices to the community. This becomes even more important as new companies enter the hydrogen market creating a growing need for hydrogen safety and reliability experts.

High-pressure hydrogen component failure has a direct negative impact on the safety and cost-effectiveness of hydrogen facilities. Premature failures increase facility maintenance cost, facility downtime, and facility size because of potentially overly conservative setback requirements. The risks associated with such leaks are not well characterized because of a lack of hydrogen specific failure rate and failure mode data [3]. In collaboration with the University of Maryland (UMD), NREL has been developing reliability capabilities for hydrogen fueling facilities which includes development of frameworks and modeling for quantitative risk assessment, prognosis health management, and industry engagement to obtain hydrogen specific risk and reliability data [4], [5].

The research team is working to understand how often and with what severity component failures occur in hydrogen systems. Components in a hydrogen equipment enclosure (HEE) may experience various failure modes that are relevant to creating the conditions whereby the system failures lead to release of hydrogen into the enclosure. Modeling well defined leak scenarios using HyRAM [6] and other risk assessment tools provides an opportunity to identify risk mitigation strategies. HyRAM contains a set of relevant component failure modes and associated probabilities for leaks from compressors, leaks from

cylinders, leaks from valves and tubing, and more. Additional failure modes are possible for these components, including failure to shutdown [7]. Further research activities occurring at NREL and UMD are developing more robust data collection structures which would enable developing necessary component failure data for all the equipment and component types inside the enclosure. [7].

Hydrogen safety sensors are a common method of risk mitigation tool and are required in certain installations, like hydrogen equipment enclosures (HEE) by codes and standards. Although required by code, guidance on optimal hydrogen safety sensor placement is limited. Hydrogen safety sensors continue to be a valuable tool to meet both code requirements of NFPA 2 [8], CHIC [9], and the International Fire Code [10], and also meet Safety Integrity Levels (SIL) of hydrogen facilities or equipment. When properly specified, maintained, and deployed hydrogen safety sensors provide an easily interpreted electrical signal which provides clear information on the state of the hydrogen facility and can be easily integrated into a facilities safety response system. Unfortunately, the location and detection threshold of hydrogen safety sensors are an afterthought in the design process. As shown by the earlier work by Tchouvelev et. Al optimal sensor placement enabling earlier leak detection and response can provide significant risk mitigation [11].

Previously AVT & Associates and NREL collaborated to develop risk mitigation guidance for sensor placement inside mechanically ventilated enclosures [11]. A critical outcome of the previous work effort was the development of science-based recommendations for updating the HEE protection table in NFPA 2:2020. These recommendations were developed based on CFD modeling results of leaks parameters recommended by IEC standard 60079-10-1 and statistical analysis [12]. The recently performed work at NREL, as part of the Component Reliability project, to quantify hydrogen leak rates from various components that failed in the field presents an opportunity to compare H2 accumulation from such leaks with previously obtained results. New data shall be used to update previous recommendations for incorporation into NFPA 2 and is thus direct contribution to dissemination of the recommendations for HHE protection requirements. Thus, the goal of the current phase 2 work task presented in this paper is: *Perform CFD modeling of characterized leaks under various ventilation conditions and leak directions in mechanically ventilated enclosures and document all activities in this task*. This task builds on the approach from the previous subcontract analyzing hydrogen dispersion in HEEs. Phase 2 of this work brings together hydrogen experts from AVT and Associates, National Renewable Energy Laboratory, and the University of Maryland. This study is highlighted in the ICHS 2023 paper by Groth et al, "Overview of International Activities in Hydrogen System Safety in IEA Hydrogen TCP Task 43" as a case study that aligns with the goals of IEA Hydrogen Task 43, Subtask E Hydrogen System Safety [13].

2.0 LEAK RATE QUANTIFICATION MEASUREMENT

2.1 Introduction of the Leak Rate Quantification apparatus

The NREL team has developed a Leak Rate Quantification Apparatus (LRQA) to support the Component Reliability project. The LRQA has been designed to quantify the leak rates of actual hydrogen components which have failed in service at pressures up to 87 MPa [4], [5]. Most standard components (e.g., valves, instruments, and fittings) can be installed in this system for testing. As shown in Fig. 1, the failed component or device under test is installed top of a 10-foot tall tower and is shielded. The purpose of this design is to protect system operators and locate leaks in a similar manner to a hydrogen vent. The LRQA cart is at the base of the tower. For leak rate quantification, equations of state using pressure, volume, and temperature, which are built into EES, are used to determine the mass flow rate of the leak at each timestep [14]-[17]. The mass flow rate can be related to an equivalent office diameter using the standard equations from ISO 9300: *Measurement of Gas Flow by Means of Critical Flow Venturi Nozzles* [18]. For leaks where the geometry is unknown, all components except calibration orifices, the discharge coefficient was assumed to be 0.9 based on typical values that are listed in ISO 9300. A more complete review of the calculations and the testing methodology was previously presented in the ICHS 2021 conference proceedings [5]. Pressure and temperature instrumentation are located at both the 1.15 L tank at the base of the tower and at the top of the tower where the device under test

(DUT) is located. The LRQA is isolated from the bulk hydrogen supply by double block and bleed valves.

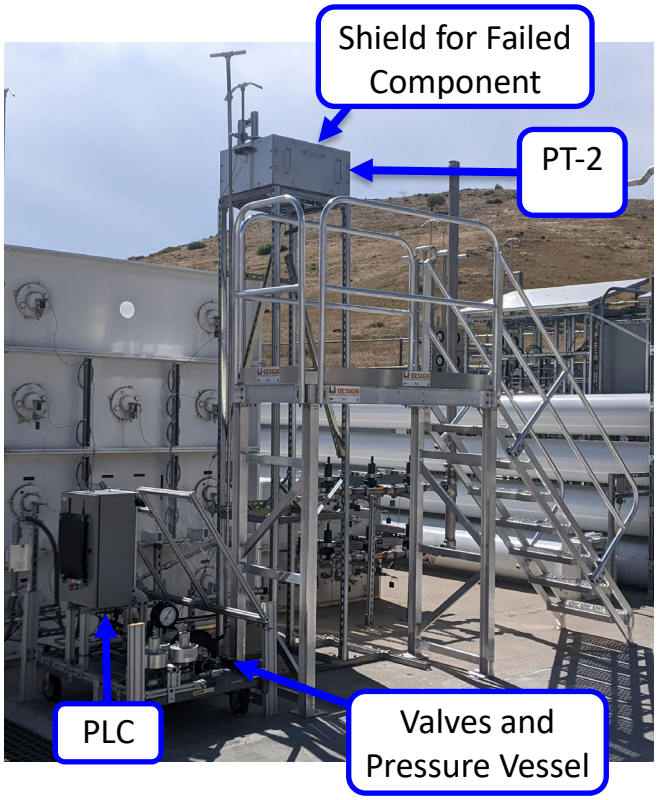

Figure 1. Leak Rate Quantification Apparatus installed at NREL. Credit: Kevin Hartmann NREL

2.2 Leak Rate Quantification Results

Testing with the LRQA provides a snapshot into the different types of failures and the associated failure rates of different components. This testing is a mechanism to highlight the issues associated with leaking hydrogen components. Although at this time not enough testing has been done to draw statistical conclusions about leak rates and the types of failures seen in hydrogen components it provides a basis which can be used to promote tracking of component failures to enable risk and reliability engineering. One example is testing which has been completed on a ball valve found to be leaking in service at NREL hydrogen fueling station. This ball valve was removed from service and tested with the LRQA. In use this ball valve was an emergency shut off valve on the supply line to a 70 MPa dispenser. The ball valve was pressurized to 82 MPa with hydrogen and initially no or a negligible leak rate was detected. Then the leak initiated and rapidly depressurized the system. The calculated orifice of the leaking ball valve is shown on the left side of Fig. 2. Due to the leak size and size of the supply buffer chamber the number of data points are limited. Additional testing was completed using pressures of 0.5 MPa to limit the leak rate and log more data points over the leak duration. This test data is shown on the right side of Fig. 2 below.

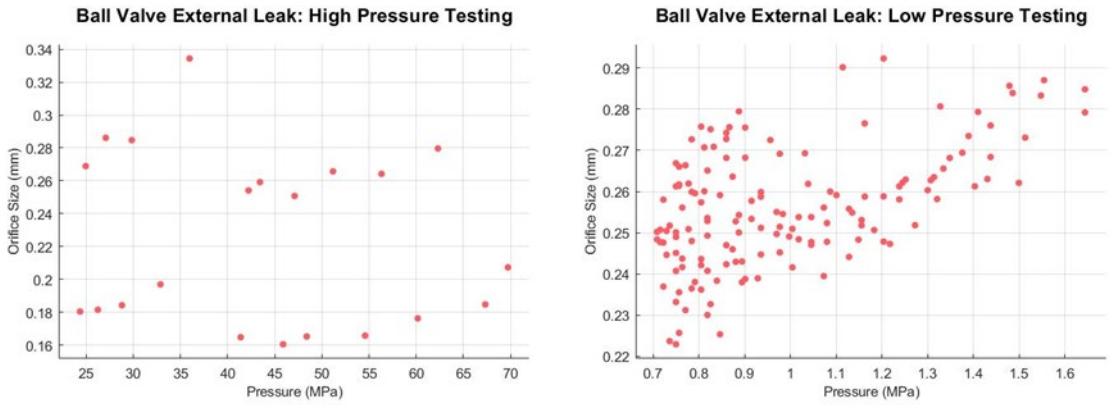

Figure 2. Leak rate quantification results from a failed ball valve a high (left) and low (right) pressure.

Although the pressure supplied to the failed component was significantly lower, the calculated average orifice was withing 0.03 mm of the high-pressure testing. The failure mode of this ball valve was an external leak due to O-ring failure. In fact, the O-ring was partially extruded from the component following testing in the LRQA.

NFPA 2 [8] and the IEC [12] both provide references to potential failure orifice sizes. NFPA 2 references 1% of the flow area of the largest tubing in a system as a leak area estimate. The NFPA 2 leak estimates have been used to help develop the NFPA 2 setback distances for hydrogen systems. This estimate is based upon feeder data from other industries and is expected to capture >95% of all leaks. IEC has taken a different approach to estimated leak sizes and provides a table which has potential leak sizes for different times of components and fittings. The leaking ball valve that was tested in the LRQA has 3/8-inch (9.525 mm) medium pressure cone and thread fittings. Therefore, using the method for leak estimating outlined in NFPA 2 for 3/8-inch (9.525 mm) outer diameter and 0.203 inch (inner diameter medium pressure tubing, most failed components will have a leak orifice diameter of 0.52 mm or less. The IEC also provides a leak estimate for a small-bore connection, under sealing elements on fixed parts, for conditions where the release opening will not expand to be 0.18 mm to 0.36 mm and between 0.36 mm and 0.56 mm for conditions where the release opening may expand. The ball valve failure with an average calculated orifice size of 0.25 mm falls within these estimates. The two additional leaks sizes used in orifice testing on the LRQA and in the modeling outlined below align well with the IEC estimates of a typical non expanding leak (0.18 mm), partially expanded leak (0.25 mm), and expanded leak (0.358 mm). To obtain a better understanding of the hazard associated with this type of leak in a hydrogen equipment enclosure modeling has been completed using data obtained from these actual failed components and orifices. This work, outlined below, demonstrates the impact of ventilation, detection, on hazard and hazard mitigation.

3.0 SELECTED ENCLOSURE GEOMETRY AND MODELING FRAMEWORK

The modeling effort described in this paper builds on the approach from previously published efforts analyzing the hydrogen dispersion inside a “large” typical 40-ft ISO container storage module [11]. The results of this CFD model can be connected to HyRAM via code coupling, or furthermore could be integrated into HyRAM. The resulting analysis will be used to inform the next edition of NFPA 2 in regard to the use of mechanical ventilation and hydrogen detection inside outdoor storage modules. Current ongoing CFD modeling of hydrogen leaks from failed components will be compared to the previously obtained results from the phase 1 work done by Tchouvelev et. al. to see if they follow the same trend [11]. If suitable similarity is identified, this would be a good demonstration that ventilation and detection requirements can be suitability informed with and thus can be predicted using engineering tools like HyRAM.

As reported in the previous published modeling effort, the large enclosure for this task was selected based on available facility in Toronto, Canada. The key components of the enclosure are shown in Fig. 3.

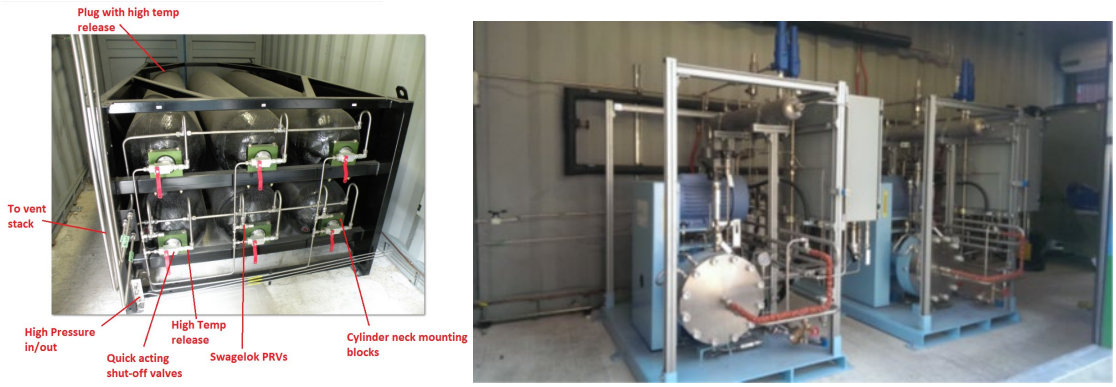

Figure 3. Key components of selected large enclosure (typical 40-ft container): HP H2 storage skid. Credit: Andrei V. Tchouvelev (ref. Canadian Tire Pilot Project).

As shown on Fig. 4, inside a 40' standard ISO container (12 m x 2.4 m x 2.4 m), two leaks were considered. Leak 1 originates from the storage units while Leak 2 originates from a valve (V-304) along the back wall of the container as shown on Fig. 3. The container is ventilated using a 595 CFM flow set at the top vent. This ventilation rate (595 CFM) is equivalent to 14.63 air changes per hour (ACH) for this enclosure. For each leak position, three leak diameters were considered: 0.18 mm, 0.25 mm, and 0.358 mm. The leak parameters used at leak location 1 and 2 are specified in Tables 1. Only one leak is active at a time. These three leak sizes were selected based on testing at NREL using the LRQA. These three leak sizes are based on the calculated orifice size of a real leaking component (see Fig. 2) or representative testing with an adjustable orifice. The pressure of 550 barg was selected as a representative pressure range based on NREL leak characterization testing data. 550 barg is also a realistic pressure for the type of storage and compressor installed in the modeled HEE. For each leak, multiples release directions were considered either horizontal or vertical along the various axis.

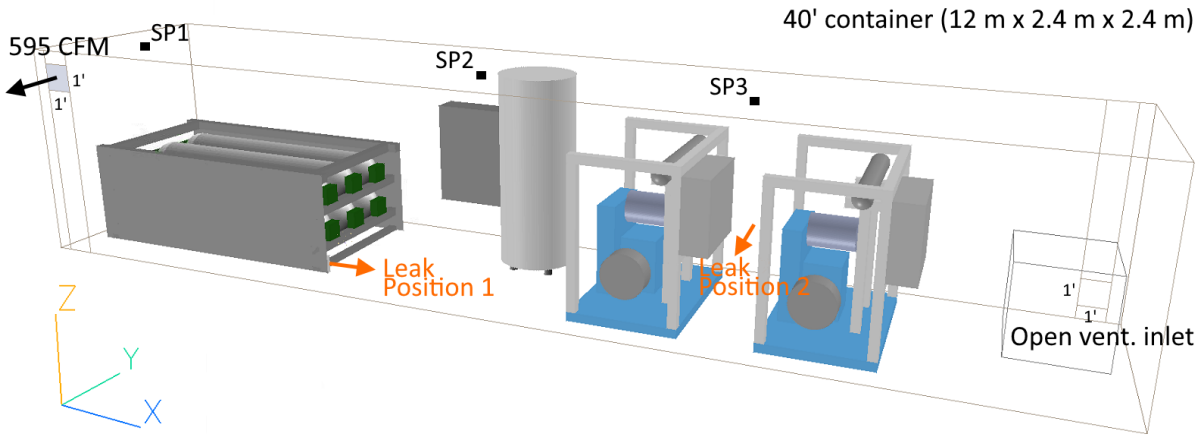

Figure 4. 40' ISO container geometry with storage, compression units, chiller, control board and ventilation openings.

Table 1. 550 barg leak parameters using ideal gas equation of state and Birch 1984 [19] notional nozzle model for Leak 1 and Leak 2 positions.

	Leak A	Leak B	Leak C
Internal Pressure (barg)	550	550	550
Circular leak diameter (mm)	**0.180**	**0.250**	**0.358**
Notional nozzle diameter (mm)	3.19	4.43	6.35
Notional nozzle area (mm^2)	7.999	15.431	31.643
Steady state mass flow rate (g/s)	**0.875**	**1.688**	**3.462**

In order to track hydrogen dispersion in real time, three virtual monitor points were installed inside the modelling domain at the locations indicated in Table 2. These three virtual monitoring points are also shown in Fig. 4 and are labelled as SP1, SP2, and SP3.

Table 2: Monitor point positions (m) for enclosure and coordinate system in Fig. 4)

Monitor point	Position (m)		
	X	Y	Z
SP1	0.30	1.20	2.10
SP2	4.45	2.10	2.10
SP3	8.00	2.10	2.10

4.0 RESULTS

Different leak scenarios were modelled using a single unidirectional leak source. The leak direction changed based on what were there realistic component leak directions. Note that for leak position 2, this did not include a leak impinging towards the back wall of the enclosure (Y-). Furthermore, the mechanical (forced) ventilation was varied between no ventilation (0 CFM) and 595 CFM for each configuration; these flow rates are above the passive ventilation achieved by the open vents. As elucidated in previous work, 595 CFM is a calculated value to ensure the background concentration does not exceed 25% LFL for estimated leak size at the nominal pressure per requirements of IEC 60079-10-1 standard [11], [12]. These different release scenarios provide system boundaries to demonstrate the impact of mechanical ventilation and leak size on the hydrogen concentration at the three virtual monitoring points within the HEE. Table 3 provides the hydrogen mole fraction at each monitoring point and each release scenario 5 hours after leak initiation. After 5 hours, the hydrogen concentration in the HEE has reached steady state and represents a scenario where the safety system (sensor or mass loss alarm) has not isolated the system form bulk storage.

Table 3: Mole fraction of hydrogen at each monitor point on the ceiling 18,000 sec (5 hours) after the onset of the leak.

Leak Position	Leak Diameter (mm)	Leak Directions	Mechanical Ventilation (CFM)	Mole fraction 18,000 sec after onset of leak (%)		
				SP1	SP2	SP3
Pos. 1	Leak A (0.18)	Horizontal X+	0	12.43	12.46	12.43
			595	5.39	5.39	5.36
		Vertical Z+	0	11.43	11.36	11.45
			595	4.36	4.45	4.65
	Leak B (0.25)	Horizontal X+	0	18.13	18.15	18.09
			595	8.87	8.83	8.78
		Vertical Z+	0	17.92	17.87	18.00
			595	8.46	8.50	8.74
	Leak C (0.358)	Horizontal X+	0	26.37	26.36	26.49
			595	16.30	16.33	16.30
		Vertical Z+	0	26.54	26.54	26.65
			595	17.55	17.32	17.70
Pos. 2	Leak A (0.18)	Horizontal Y-	0	11.80	11.91	11.94
			595	5.71	5.78	5.77
		Vertical Z+	0	11.67	11.56	11.40
			595	4.42	4.31	4.44
		Vertical Z-	0	11.64	11.96	11.54
			595	4.53	4.76	4.19
	Leak B (0.25)	Horizontal Y-	0	17.65	17.78	17.73
			595	10.57	10.70	10.61
		Vertical Z+	0	17.46	17.42	17.29
			595	8.56	8.48	8.71
		Vertical Z-	0	17.13	16.85	16.70
			595	7.22	6.30	5.39
	Leak C (0.358)	Horizontal Y-	0	27.23	27.48	27.36
			595	17.68	17.89	17.77
		Vertical Z+	0	26.12	26.11	25.46
			595	17.60	17.57	16.95
		Vertical Z-	0	26.47	26.40	24.89
			595	14.68	13.05	12.78

Table 3 provides the hydrogen concentration at each monitoring location but provides limited input as to the mass of hydrogen at flammable concentrations within the HEE. It is clear that in all scenarios a portion of the enclosure has reached the lower flammability limit of the hydrogen, 4% mole fraction. CFD modelling provides an overall assessment of the mass and volume of hydrogen at a flammable concentration in the HEE as shown for a Leak C (0.358 mm) scenario in Fig. 5. The leak scenarios plotted in Fig. 5 are highlighted by the bold box in Table 3 and Table 4. This type of modelling can be leveraged with quantitative risk assessment to make data-driven decisions to mitigate risk, which is a future goal of this effort. As outlined in Fig. 5, Position 1, Leak C (0.358), Horizontal X+, No Ventilation, there is less than 0.1 kg of hydrogen at the 4% - 75% mole fraction before 58.7 seconds. Similarly, there is only 0.1 kg of hydrogen at the 8% - 75% mole fraction after 117.1 seconds. There is time for a well-placed safety sensor to detect the leak and initiate the safety system. Fig. 5 also demonstrates how forced ventilation in the enclosure plays a role in the dilution of the flammable gas,

increasing the time required to achieve a significant cloud of flammable gas and slowing the rate at which the flammable mass increases.

Position 1 Leak C (0.358 mm) Hor. X+ No Mech. Ventilation	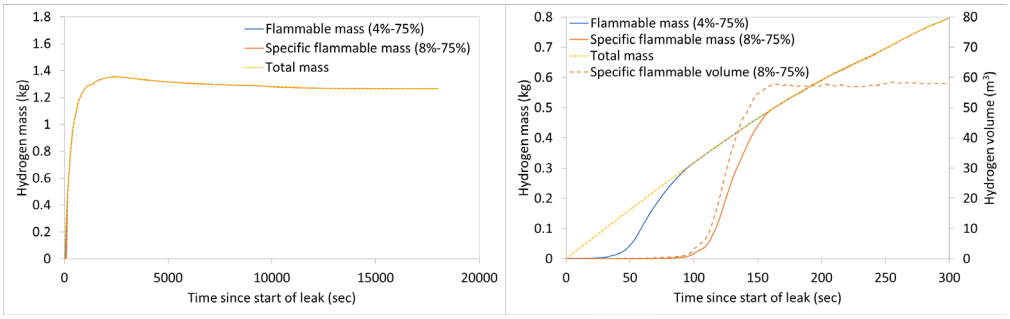
Position 1 Leak C (0.358 mm) Hor. X+ 595 CFM	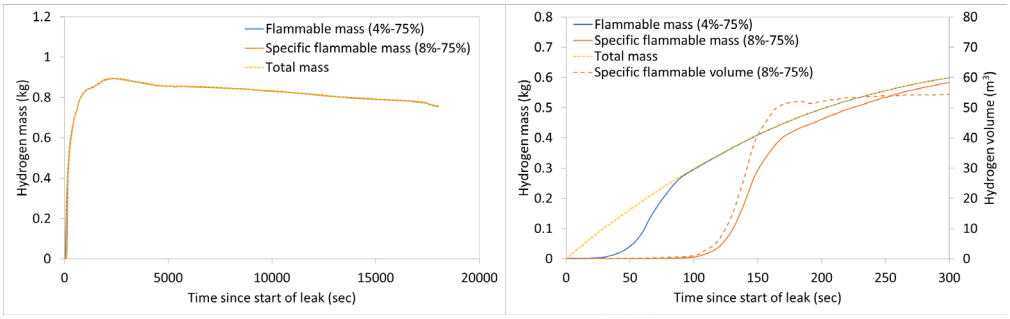
Position 1 Leak C (0.358 mm) Vertical Z+ No Mech. Ventilation	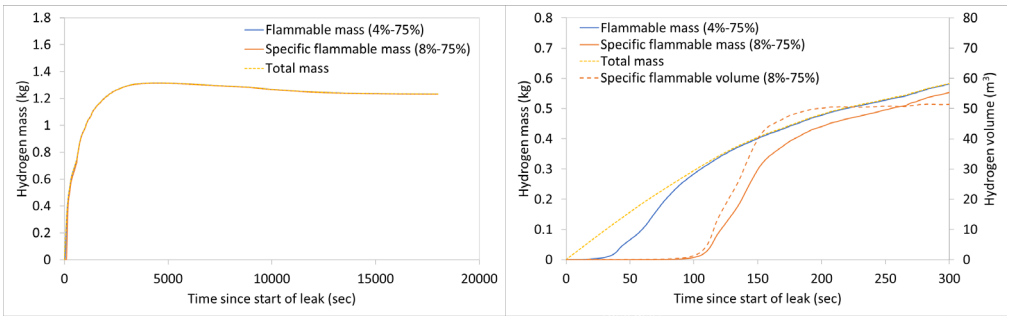
Position 1 Leak C (0.358 mm) Vertical Z+ 595 CFM	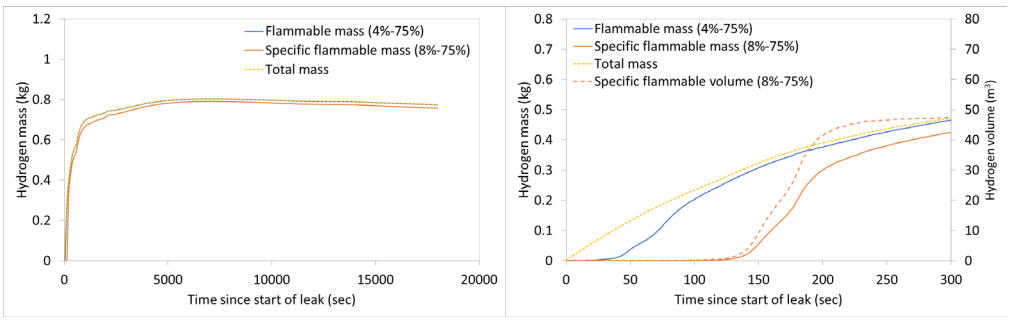

Figure 5. For Leak position 1, flammable (4%-75% mole fraction), specific (8%-75% mole fraction) and total hydrogen mass (kg) as well as specific (8%-75% mole fraction) flammable volume (m^3) (estimated using Amagat's law with SP2 concentrations) inside enclosure for a 18,000 sec (5 hours) leak. For the cases with mechanical ventilation, the leak starts at 600 sec.

To mitigate the hazard associated with hydrogen accumulation in a HEE, it is critical to minimize the time to detection. Although NFPA 2 requires detection of >1% mole fraction (25% LFL) in the HEE to trigger the Emergency Shutdown System [8], as discussed in the previous phase of this work a lower-level detection limit on the order of 0.1% mole fraction is recommended [11]. A lower detection limit enables earlier response to an out of normal scenario and therefore reduces the quantity of flammable mass in the enclosure prior to detection. Additionally, the sensor placement is a critical factor on the duration of the release and the mass of flammable gas once the detection limit is reached. A lower

detection provides an overall risk reduction through earlier detection and response to a leak. Table 4 highlights the time to detection at a level of 0.1% mole fraction if hydrogen safety sensors are deployed in a HEE at the three different virtual monitoring points. For all leak scenarios the longest time to detection is 47.4 seconds at virtual monitor SP1, leak position 1, leak size A (0.18 mm), horizontal X+ direction, and with no ventilation. This is still significantly less than the time required to have greater than 0.1 kg of hydrogen at the flammable concentration of 4% - 75% (267.6 sec) or the specific flammable concentration of 8% - 75% (832.6 sec) for this same release. Detection location SP2 and SP3 both had detection times of less than 24 seconds in the same leak scenario. This information is critical for risk mitigation through optimal sensor placement to reduce detection time.

Table 4: Detection time (sec) for hydrogen at a concentration of 0.1% mole fraction to reach each monitor point on the ceiling.

Leak Position	Leak Diameter (mm)	Leak Directions	Mechanical Ventilation (CFM)	Detection time to reach 0.1% mole fraction after onset of leak (sec)		
				SP1	SP2	SP3
Pos. 1	Leak A (0.18)	Horizontal X+	0	47.4	23.7	17.8
			595	39.8	20.3	15.0
		Vertical Z+	0	9.3	3.4	12.3
			595	7.6	3.6	14.2
	Leak B (0.25)	Horizontal X+	0	35.6	19.0	14.6
			595	31.0	16.2	12.5
		Vertical Z+	0	6.5	2.4	8.9
			595	5.6	2.6	10.1
	Leak C (0.358)	Horizontal X+	0	25.1	14.2	10.4
			595	22.1	13.2	10.0
		Vertical Z+	0	4.4	1.7	6.2
			595	4.0	1.7	6.9
Pos. 2	Leak A (0.18)	Horizontal Y-	0	24.3	11.1	9.2
			595	20.7	10.8	9.26
		Vertical Z+	0	19.5	21.7	28.4
			595	19.0	22.6	26.6
		Vertical Z-	0	24.4	9.0	12.7
			595	21.3	8.9	12.6
	Leak B (0.25)	Horizontal Y-	0	17.4	8.4	6.8
			595	15.3	8.1	6.9
		Vertical Z+	0	15.0	17.8	24.5
			595	15.2	18.7	25.6
		Vertical Z-	0	16.8	7.2	9.7
			595	15.4	7.2	9.9
	Leak C (0.358)	Horizontal Y-	0	11.9	6.2	4.8
			595	10.9	6.0	4.9
		Vertical Z+	0	11.4	14.4	19.5
			595	12.0	14.9	17.5
		Vertical Z-	0	11.3	5.6	7.1
			595	10.3	5.6	7.4

5.0 CONCLUSION

Based on the considered leak scenarios, the mechanical ventilation setup of this enclosure and air flow rate are sufficient to prevent accumulation of hazardous flammable amount of hydrogen even for extended / exaggerated leak duration for the unexpanded leak of 0.18 mm, but not the expanded leaks of 0.25 mm and particularly 0.385 mm. Hydrogen concentrations due the leaks from the largest expanded orifice can reach 17% vol. at the monitor points in the extended 18,000 second leak scenario. At the same time, without mechanical ventilation hydrogen accumulates to hazardous levels above 8% mole fraction in the entire enclosure for all leaks sizes, and for 0.358 mm, where hydrogen concentrations can reach very hazardous 27% range, which is very close to stoichiometry. Particularly important is the amount of flammable mass in the HEE. In the case of no mechanical ventilation the amount of flammable mass is 50% higher than in the case with mechanical ventilation as shown on Fig. 5. Coupled with lower concentration, the reduced flammable mass presents a significantly lower hazard than the case with no mechanical ventilation. Natural (passive) ventilation is thus insufficient to deal with any of the considered leak scenarios in the specified geometry and locations of air intake and exhaust. Although most of the considered leak scenarios can be detected within 15 s under no mechanical ventilation condition (with a few cases where it may take slightly longer), in the case when the leak continues after the system shutdown under no mechanical ventilation condition, the average hydrogen concentration can exceed 8% mole fraction within 150 s after the onset of the leak, which can lead to a very hazardous situation.

This study demonstrates that mechanical ventilation in combination with early detection play a critical role in mitigating hazards associated with the leaks from hydrogen piping and components. Placement of sensors, detection time, and control system response time also play a critical role in minimizing the flammability hazard in connection with mechanical ventilation.

5.1 Impact of Leak Direction

The graphs on Fig. 5 also provide an insight on the relevant significance of the leak direction depending on the leak location and the setup of the ventilation, i.e., the locations of inlet and outlet. For example, for the position 1 for the expanded leak of 0.358 mm, leak in the horizontal direction results in noticeable increase of the flammable mass vs the vertical direction from the same position: e.g., 0.8 kg (horizontal) vs 0.6 kg (vertical) for “no ventilation case” and 0.55 kg (horizontal) vs 0.45 kg (vertical) for the case with mechanical ventilation. This indicates that having just one inlet opening may not be enough for the air intake if there is a good chance that horizontal leaks may get into a dead space of the HEE. Future work will investigate the impact of the ventilation configuration including the number of ventilation inlets.

5.2 QRA Moving Forward

Recognizing that different system configurations may be more or less likely to result in releases into the enclosure, near-term next steps for this work are to develop additional aspects of the QRA models that can be used to model total system risk, as illustrated in [20]. Our next steps include developing the risk scenario models and equipment failure logic models (e.g., event tree, fault tree) of QRA for the equipment inside the enclosure and connecting those to these consequence simulations. With more specific analysis of the hydrogen equipment in Fig. 3 and Fig. 4, we could develop QRA models for the system to identify probability of failures, probability of undesired outcomes, and calculate total risk to the populations and facilities of interest in the NFPA 2 and compare that risk to similar systems and/or established risk tolerability metrics. Extending the work to include equipment and failure logic models provides the potential to gain insights into the relative risk posed by the system, using QRA to assess risk across a wider spectrum of potential release scenarios and outcomes. Furthermore, the fault tree and important measure aspects of QRA can be used to gain insight into ways to reduce the probability of leaks and releases from the hydrogen equipment in the enclosure. An end-to-end analysis can demonstrate how providing multiple layers of protection can together further minimize the probability

and magnitude of the hazards. Ongoing work to connect these results into multiple facets of NFPA 2 and ISO 19880-1 should be explored.

6.0 ACKNOWLEDGMENTS

This work was authored in part by the National Renewable Energy Laboratory, operated by Alliance for Sustainable Energy, LLC, for the U.S. Department of Energy (DOE) under Contract No. DE-AC36-08GO28308. Funding provided by the U.S. Department of Energy Office of Hydrogen and Fuel Cell Technologies Office. The views expressed in the article do not necessarily represent the views of the DOE or the U.S. Government. The U.S. Government retains and the publisher, by accepting the article for publication, acknowledges that the U.S. Government retains a nonexclusive, paid-up, irrevocable, worldwide license to publish or reproduce the published form of this work, or allow others to do so, for U.S. Government purposes.

7.0 REFERENCES

1. "Hydrogen and Fuel Cell Technologies Office Multi-Year Research, Development, and Demonstration Plan," U.S. Department of Energy, 2015.
2. "Hydrogen Shot," U.S. Department of Energy, Accessed March 30, 2023. [Online]. Available: https://www.energy.gov/eere/fuelcells/hydrogen-shot.
3. M. West, A. Al-Douri, K. Hartmann, W. Buttner, and K. M. Groth, "Critical Review and Analysis of Hydrogen Safety Data Collection Tools," *International Journal of Hydrogen Energy*, vol. 47, no. 40, pp. 17845–17858, May 2022, doi: 10.1016/j.ijhydene.2022.03.244.
4. K. Hartmann, A. Al-Douri, J. Thorson, W. Buttner, K. Groth, "Component Reliability R&D," *Presented at 2022 DOE Hydrogen Fuel Cell and Technologies Office Annual Merit Review,* Virtual, June 2022.
5. K. Hartmann, C. Correa-Jullian, J. Thorson, K. Groth, W. Buttner, "Hydrogen Component Leak Rate Quantification for System Risk and Reliability Assessment Through QRA and PHM Frameworks," *Proceedings of International Conference on Hydrogen Safety (ICHS 2021)*, Virtual, Sep. 21-24, 2021.
6. B. D. Ehrhart, C. Sims, E. S. Hecht, B. B. Schroeder, K. M. Groth, J. T. Reynolds, and G. W. Walkup, "HyRAM+ (Hydrogen Plus Other Alternative Fuels Risk Assessment Models) Version 5.0," Sandia National Laboratories, November 2022. [Online]. Available: https://hyram.sandia.gov.
7. K. Groth, A. Al-Douri, M. West, K. Hartmann, G. Saur, W. Buttner, "Design and Requirements for a Hydrogen Component Reliability Database (HyCReD)," International *Journal of Hydrogen Energy,* Submitted March 2023.
8. NFPA 2, *Hydrogen Technologies Code,* National Fire Protection Association 2023.
9. CAN/BNQ1784-000, Canadian Hydrogen Installation Code (CHIC), 2007.
10. International Fire Code (IFC), International Code Council, 2015.
11. A. V. Tchouvelev, W. J. Buttner, D. Melideo, D. Baraldi, and B. Angers, "Development of risk mitigation guidance for sensor placement inside mechanically ventilated enclosures – Phase 1," *International Journal of Hydrogen Energy*, vol. 46, no. 23, pp. 12439–12454, March 2021, doi: https://doi.org/10.1016/j.ijhydene.2020.09.108.
12. IEC 60079-10-1, *Explosive Atmospheres – Part 10-1 Classification of Areas – Explosive Gas Atmospheres,* International Electrotechnical Commission, 2020.
13. K. Groth et al, "Overview of International Activities in Hydrogen System Safety in IEA Hydrogen TCP Task 43," *Proceedings of International Conference on Hydrogen Safety (ICHS 2023)*, Quebec, Sep. 19-21, 2023.
14. D. O. O. Vega, "A New Wide Range Equation of State for Helium-4," PhD Thesis, Chemical Engineering Texas A&M University, 2013.

15. J. W. Leachman, R. T. Jacobsen, S. G. Penoncello, and E. W. Lemmon, "Fundamental Equations of State for Parahydrogen, Normal Hydrogen, and Orthohydrogen," *Journal of Physical and Chemical Reference Data,* vol. 38, no. 3, pp. 721, 2009, doi: https://doi.org/10.1063/1.3160306
16. R. Span, E. W. Lemmon, R. T. Jacobsen, W. Wagner, and A. Yokozeki, "A Reference Equation of State for the Thermodynamic Properties of Nitrogen for Temperatures from 63.151 to 1000 K and Pressures to 2200 MPa," *Journal of Physical and Chemical Reference Data*, vol. 29, no. 6, pp. 1361-1433, 2000. https://doi.org/10.1063/1.1349047
17. S. A. Klein, "EES – Engineering Equation Solver, Version 10.934-3D, 2020-10-06," F-Chart Software, [Online]. Available: http://fchartsoftware.com.
18. "ISO 9300 Measurement of gas flow by means of critical flow Venturi nozzles." International Organization for Standards (ISO), 2005, [Online]. Available: https://www.iso.org/standard/34272.html
19. A. D. Birch, D. R. Brown, M. G. Dodson, F. Swaffield, "The Structure and Concentration Decay of High Pressure Jets of Natural Gas," *Combustion Science and Technology,* vol. 36, no. 5-6, pp. 249-261, 1984. doi: https://doi.org/10.1080/00102208408923739
20. A. Al-Douri, A. Ruiz-Tagle, and K. M. Groth, "A Quantitative Risk Assessment of Hydrogen Fuel Cell Forklifts," *International Journal of Hydrogen Energy*, Feb. 2023, doi: https://doi.org/10.1016/j.ijhydene.2023.01.369